viruses

MDPI

Type of the Paper (Article)

Darunavir Resistant HIV-1 Protease Constructs Uphold a Conformational Selection Hypothesis for Drug Resistance

Zhanglong Liu[1, a)], Trang T. Tran[1)], Linh Pham[1, b)], Lingna Hu[1)], Kyle Bentz[1, c)], Daniel A. Savin[1)], and Gail E. Fanucci[1, *)]

[1]Department of Chemistry, University of Florida, Gainesville, 32611.
[a] Current address: LinkedIn, Mountain View, CA, USA
[b] Current address: Department of Science and Mathematics, Texas A&M University - Central Texas, Killeen, TX 76549, USA.
[c] Current address: Department of Chemistry and Biochemistry, University of California, San Diego,La Jolla, California 92093; United States
* Correspondence: fanucci@chem.ufl.edu; Tel.: 352-392-2345; Fax: 352-392-0872

Received: date; Accepted: date; Published: date

Abstract: Multidrug resistance continues to be a barrier to the effectiveness of highly active antiretroviral therapy in the treatment of Human immunodeficiency virus 1 (HIV-1) infection. Darunavir (DRV) is a highly potent protease inhibitor (PI) that is oftentimes effective when drug resistance has emerged against first generation inhibitors. Resistance to darunavir does evolve and requires 10-20 amino acid substitutions. The conformational landscape of six highly characterized HIV-1 protease (PR) constructs that harbor up to 19 DRV-associated mutations was characterized by distance measurements with pulsed electron paramagnetic resonance spectroscopy, namely double electron-electron resonance (DEER). Results show that the accumulated substitutions alter the conformational landscape compared to PI-naïve protease where the semi-open conformation is destabilized from the dominant position with open-like states becoming prevalent in many cases. A linear correlation is found between values of the DRV inhibition parameter K_i and the open-like to closed state population ratio determined from DEER. The nearly 50% decrease in occupancy of the semi-open conformation is associated with reduced enzymatic activity characterized previously in the literature.

Keywords: HIV-1 protease; darunavir; genetic and phenotypic diversity, DEER spectroscopy, drug resistance

1. Introduction

HIV-1 protease (PR) is a potent target in the treatment of HIV-1 infection because its inhibition leads to non-infectious immature virus particles [1-5]. Protease inhibitors in combination with other classes of anti-HIV drugs given in antiretroviral therapies (ARTs) are very successful in keeping viral loads below detectable limits within the blood. However, the emergence of multidrug resistance is a roadblock to the successful suppression of undetectable viral loads in infected patients and as such there is great interest in understanding mechanisms of drug resistance [6-8].

Our lab has utilized distance measurements from pulsed electron double resonance (PELDOR) paramagnetic resonance spectroscopy, also commonly referred to as double electron-electron resonance (DEER) spectroscopy[9-11], to formulate a conformational landscape hypothesis for how mutations combine to impact drug resistance and restore kinetic fitness in HIV-1 PR. In our model we postulate that drug-pressure selected mutations combine to stabilize open-like states (either wide-open or curled-open) and destabilize closed-like conformations [12-19] The conformational sampling scheme encompasses four conformational ensembles described as curled-open, wide-open, semi-

open and closed. (Figure 1) These conformations have been evoked from a combination of X-ray structures, molecular dynamic simulations and our pulsed EPR data[19, 20]. Our prior work has also shown that as the open-like conformations become more highly populated, overall protein backbone dynamics increases [16, 19]. This conformational selection hypothesis can be operating in addition to drug-resistance produced by other mechanisms including structural alterations to the binding site cavity, distal mutations that alter dimerization/subunit interactions, gag/pol substrate processing, and protease dynamics [21-29].

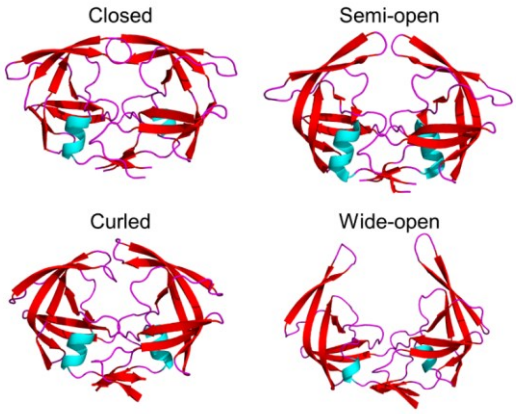

Figure 1. Four representative conformations of populations to describe the HIV-1 PR conformational landscape, namely closed (PDBID: 2BPX), semi-open (PDBID: ~~1TW7~~), curled (MD coordinates) and wide-open (MD coordinates). Color coding represents different secondary structural elements with cyan, red and magenta showing helical, sheet and random coil; respectively.

Commented [FE1]: Trang, please see comments to you on reviewer's comments. I am asking you to remake this figure.

One of our earlier studies focused on the specific accumulation of amino acid changes in response to Nelfinavir (NFV) treatment, specifically the D30N primary mutation with accumulation of secondary mutations M36I and A71V [14, 30]. We also investigated the impact of accumulated mutations in three clinical isolate sequences that demonstrated multi-drug resistance [12, 13, 15, 18]. Here we extend the investigation to a set of Darunavir (DRV) resistant sequences that were generated via analysis of mutated clinical derived sequences from subtype B [31]. Darunavir is the most recently approved HIV-1 PR inhibitor and it shows a high genetic barrier to resistance [32]. However, resistance has been clinically reported and understanding mechanisms for resistance is important for early detection of treatment failure and design of next generation PIs capable of inhibiting multidrug resistant virus [28, 33-43].

The sequences of HIV-1 PR targeted for this study are given in Figure 2 and the location of the amino acid changes are shown as spheres on ribbon diagrams. Kinetic and inhibition parameters have been previously characterized for these constructs [31]; structural information also exists for these or other DRV resistant constructs [44-46]. Thus, they readily provide a set of constructs to add to our postulated model of conformational selection for understanding multidrug resistance and enzymatic activity. DRV-resistance oftentimes results in > 18 amino acid changes, and these constructs represent the most highly mutated PR sequences we have investigated by pulsed EPR spectroscopy to date. Our earlier work on three multidrug resistant constructs had 10, 7, and 10 mutations; respectively for constructs termed POST [12], V6 [15, 18] and MDR769 [13].

	10	20	30	40	50
Subtype B	PQITLW**K**RPL	VTIKIGGQLK	EALL**N**TGADD	TV**I**EEMSLPG	RWKPKMIGGI
DRV1	PQITLWQRPL	V**VV**K**V**GGQL**M**	EALL**N**TGADD	T**IF**EEM**N**LPG	RW**T**PKMIGGI
DRV2	PQITLWQRPL	VT**V**KIGGQL**R**	EALL**N**TGADD	T**IF**E**DI**SLPG	K**W**T**P**KM**V**GGI
DRV3	PQITLWQRP**F**	VT**V**KIGGQLK	EALL**N**TGAD**N**	TVLEEMSLPG	RWKP**I**MIGG**L**
DRV4	PQITLWQRP**I**	VT**VR**IGGQLK	EALL**N**TGADD	T**IF**EEMSLPG	RW**T**PK**IV**GGI
DRV5	PQITLWQRP**I**	VT**V**KI**E**GQLK	EALL**N**TGADD	TV**F**EE**LT**L**S**G	RWKP**RL**IGGI
DRV6	PQITLWQRP**I**	VT**V**K**V**GGQL**R**	EALL**N**TGADD	TV**FNDI**SLPG	RW**T**PKM**V**GG**L**

	60	70	80	90
Subtype B	GGFI**C**VRQYD	QI**I**IEI**A**GHK	AIGTVLVGPT	PVNIIGRNLL TQIG**A**TLNF
DRV1	GGF**LC**VRQYD	Q**VP**IEI**A**GHK	**VVS**TVL**I**GPT	P**L**N**V**IGRN**VM** TQIG**A**TLNF
DRV2	GGF**MC**VRQYD	Q**VV**IEI**A**GHK	**VTSP**VLVGPT	P**L**NIIGRN**V**L TQ**L**G**A**TLNF
DRV3	GGFI**C**VRQYD	QI**P**IEI**A**GHK	**I**IGTVL**I**GPT	PVNIIGR**D**LL TQIG**A**TLNF
DRV4	GGF**LC**VRQYD	Q**VP**IEI**A**GHK	**TTT**TVL**I**G**S**T	PVN**V**IGRNL**M** TQIG**A**TLNF
DRV5	GGF**VC**VRQYD	Q**VP**IEI**A**GHK	**VI**DTVLVGPT	PT**N**VIGRN**VM** TQ**L**G**A**TLNF
DRV6	GG**LI**C**V**RE**Y**D	Q**VP**IE**FA**GHK	**V**IGTVL**I**GPT	PA**N**VIGRN**V**L TQIG**A**TLNF

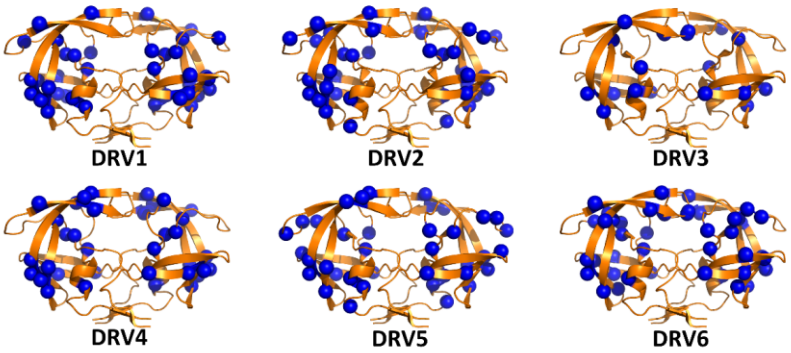

Figure 2. (Top) Graphical table showing DRV1-6 HIV-1 PR sequences with boldfaced underlined residues in blue indicating substitutions relative to PI-naïve subtype B. Blue bolded face residues in sequence of PI-naïve subtype B indicate stabilizing mutations (Q7K, L33I and L63I). Black boldfaced annotation for D25N shows these constructs contained inactivation of the catalytic site to aid in stabilization. Red boldfaced labels indicate locations modified for EPR investigations as described in Materials and Methods. (Bottom). Ribbon diagrams of HIV-1PR (pdb: 2PK5) with spheres show the locations of the amino acid substitutions in DRV1-6 relative to PI-naïve subtype B

Commented [FE2]: Trang, please remake this accordingly

Overall, the results for these DRV-resistant constructs uphold a conformational landscape model where a correlation between the ratio of the open-like to closed-like states to inhibition values are observed. This trend indicates a flip-flop in the stability of the open to closed like states; with drug-pressure selected mutations stabilizing open-like states. This seems reasonable given that current inhibitors are modeled after the transition-state analog of the substrate which binds to a closed conformation of the enzyme. Results further suggest an on-off switch for kinetic turn-over that requires the semi-open population of the unliganded enzyme to predominate (> 60% relative population) for efficient activity. Together, findings suggest the consideration of open-like conformations, and non-active-site inhibitor binding, as potential targets for novel inhibitor design strategies.

2. Materials and Methods

2.1. *Cloning and Mutagenesis*

DNA, which was mRNA stabilized and codon optimized for expression in *Escherichia coli*, that encodes for each of the DRV sequences given in Figure 2 was purchased from DNA 2.0 (Meno Park, CA). Genes were subcloned into pET-23a vectors (Novagen, Madison WI) under the control of the T7 promoter. DRV constructs included three stabilizing mutations, Q7K, L331, and L63I, which we have typically included in earlier DEER investigations of HIV-1PR, as we desired to match our protein samples as closely to those previously studied [20, 47]. These sites are omitted if one of these locations is a natural polymorphism or drug-pressure selected mutation. HIV-1PR is a homodimer, so one CYS substitution generates a pair of spin labels for distance measurements. For spin-labeling, a unique cysteine at site 55 is incorporated, which has been shown not to alter enzyme activity [48, 49], and which we have shown can be readily spin-labeled as well as tolerate a fluorescent tag without protein precipitation/aggregation [50]. We initially chose site K55C based upon analysis of all HIV-1PR structures in the PBD in 2005 analyzing distance between terminal lysine amine groups that predicted ~ 3 Å difference should be observed in our DEER data. We have demonstrated that this single spin-labeled site also reports changes in distances and distance distributions between the major conformations detected in numerous X-ray structures of closed (33Å) and open (36 Å), and we find reports well on two other conformational state of wide-open (> 40 Å) and a curled/tucked state (25-30 Å) [16, 51, 52], results have been substantiated by MD simulations [15, 53] and crystallographic investigations [16, 52]. To ensure unique labeling, the two naturally occurring cysteine residues are substituted with (C67A, C95A) which is often done in crystallographic studies to prevent disulfide bond formation and limit protein aggregation [48, 54]. To facilitate spectroscopic studies, all samples for DEER spectroscopy contain the D25N mutation, and we have shown this mutation does not impact the trends of inhibitor binding [16, 17]. The fidelity of the HIV-1 PR gene sequence was confirmed by Sanger DNA sequencing (ICBR Genomics Facility, University of Florida).

2.1. *Protein Expression, purification, and spin-labeling*

Protein was expressed as described in previous publications, with adjustment of the pH of the inclusion body buffer for anion exchange [12]. We find that the isoelectric point of HIV-1PR is altered upon amino acid substitution and we alter purification buffer pH to optimize purification conditions that prevent protein aggregation. Buffers were adjusted to pH 7.14, 8.52, 8.52, 8.55, 7.14, 8.55; for DRV1, DRV2, DRV 3, DRV4, DRV5 and DRV6; respectively. Protein was spin labeled with MTSL (1-Oxyl-2,2,5,5-Tetramethyl-Δ3-Pyrroline-3-Methyl) Methanethiosulfonate (Santa Cruz Biotechnology), freshly dissolved in ethanol, in a 5-10x excess of the protein concentration. The reaction was carried out in 10 mM Tris-HCl buffer pH 6.9 for 6-12 hours in the dark at 4°C because protease is found to precipitate if the labeling is performed at room temperature. After the reaction, excess spin-label was removed by buffer exchange into 2 mM NaOAc pH 5.0 using HiPrep 26/10 desalting columns. Spin-labeling was confirmed through mass spectrometry analysis. Accurate mass experiments were performed on an Agilent 6220 ESI TOF (Santa Clara, CA) mass spectrometer equipped with an electrospray source operated in positive ion mode. Agilent ESI Low Concentration Tuning Mix was used for mass calibration for a calibration range of m/z 100 - 2000. Samples were prepared in a solution containing acidified acetonitrile (0.5% formic acid) and 1 μL was injected into the electrospray source at a rate of 100 ml min^{-1}. Optimal conditions were capillary voltage 4000 V, source temperature 350oC and a cone voltage of 60 V. The TOF analyzer was scanned over an appropriate m/z range with a 1 s integration time. Data was acquired in continuum mode until acceptable averaged data was obtained. ESI results were collected for all samples and complete spin labeling of proteins was confirmed with correctly anticipated masses before proceeding to DEER data collection.

2.1. *Sample preparation, DEER data collection and analysis*

For DEER spectroscopy, samples were further concentrated and buffer exchanged to 100-140 μM dimer concentration in 20 mM D_3-NaOAc/D_2O, pH 5.0 with 30% v/v D_8-glycerol by buffer exchange using centrifugal membrane concentrators (Millipore, Billerica, MA). For DRV1 and DRV3 unbound HIV-1 PR, aggregation problems were encountered in the sodium acetate buffer at pH 5 as evidenced

by continuous wave (CW) X-band EPR line shapes (Figures SI2-3) [55]. Various pH conditions were explored, and homogenous protein samples (via CW EPR and dynamic light scattering (DLS) given in Supporting information) with the high concentration of around 100 μM were only obtained at pH 2.8-3.0. Our lab has performed solution NMR and X-ray crystallography of HIV-1PR in the past, so we have experience in knowing what spectroscopic signatures in CW EPR line shapes signify homogeneous samples and the Supporting DLS data helps verify sample integrity [12, 17], [19] Samples with inhibitors were prepared by adding a 4-fold molar excess of inhibitor followed by equilibration at room temperature for four hours prior to freezing in liquid nitrogen for EPR measurements. Ratio of inhibitor:PR was determined from earlier NMR titration experiments [17, 19] Inhibitors were obtained from the NIH AIDS Research and Reference Reagent Program, Division of AIDS, NIAID, NIH and the non-hydrolysable CaP2 substrate mimic (H-Arg-Val-Leu-r-Phe-Glu-Ala-Nle/NH2 (r = reduced)) was purchased from Peptides International (KY). Continuous wave (CW) EPR spectra were collected at room temperature on a Bruker E500 spectrometer with a Bruker dielectric resonator. Spectra were reported as an average of 16 scans with 100 G sweep width, 0.8G modulation amplitude, 100 kHz modulation frequency and 2 mW incident microwave power CW spectra serve as a control for sample quality prior and after DEER experiments. All DEER experiments were performed on a Bruker EleXsys E580 spectrometer at 65 K with an ER 4118X-MD5 dielectric split-ring resonator. Samples were flash frozen in liquid nitrogen before inserted into the resonator. The four-pulse DEER sequence was utilized as described previously [14, 16, 19, 56]. Distance profiles are determined by Tikhonov regularization (TKR) as implemented within DEERAnalysis2013 (http://www.epr.ethz.ch/software.html) [9, 10], [11]. Population analysis proceeds via Gaussian reconstruction and peak suppression of the DEER distance profile as outlined previously [14, 19, 56-58]. Complete details of data analysis are provided in the Supporting Information (Figures SI5-24).

3. Results

3.1. ***DRV resistant constructs sample high fractional occupancy of open-like and closed state compared to PI-naïve Subtye B.***

Because HIV-1 PR is a homodimer, incorporation of a single spin label into the protein at site K55C provides a spin-pair for distance measurements by DEER [15, 20, 48]. Figure 3 shows DEER distance profiles of spin-labeled HIV-1 PR DRV resistant constructs compared to PI-naïve subtype B (Details of data processing of DEER echo curves to generate final distance profiles is provided in Supporting Information). The data clearly reveal marked alterations in the conformational sampling landscape of these DRV resistant constructs relative to PI-naïve subtype B; particularly with a greater population of sampling distances < 30 Å, which we assign to a curled-open conformation [14, 16, 19], and distances > 40 Å, corresponding to a wide-open conformation [12, 16, 18-20, 56, 58].

Table 1 summarizes the most probable distance and the average distance observed in the DEER distance profiles in Figure 3. For unbound HIV-1PR, DRV 5 and DRV6 have most probable distances most similar to PI-naïve subtype B, whereas DRV1 and DRV2 have most probable distances markedly longer than that seen in PI-naïve subtype B, with DRV3 and DRV4 having shorter ones.

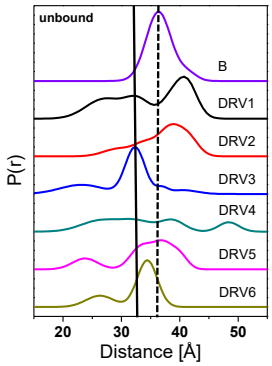

Figure 3. DEER distance probability profiles of unbound HIV-1 PR PI-naïve subtype B, DRV1, DRV2, DRV3, DRV4, DRV5 and DRV6 from top to the bottom. Profiles are area normalized to 100% probability distribution, P(r), and vertically offset for clarity. Dashed line at 36 Å represents the nominal distance observed for HIV-1PR semi-open population whereas the solid line at 33 Å signifies the nominal distance observed for the HIV-1PR closed population.

Table 1. Most probable and averaged distance from DEER distance profiles for HIV-1 DRV resistant proteases and PI-naïve subtype B.

	unbound		**CaP2**		**DRV**	
HIV-1 constructs	**Most probable distance (Å) (error ±0.2)**	**Average distance (Å) (error ±0.2)**	**Most probable distance (Å) (error ±0.2)**	**Average distance (Å) (error ±0.2)**	**Most probable distance (Å) (error ±0.2)**	**Average distance (Å) (error ±0.2)**
DRV1	40.7	34.6	36.8	35.9	38.7	34.9
DRV2	39.1	36.9	39.1	36.0	40.5	37.1
DRV3	32.2	31.6	32.6	33.3	32.6	32.7
DRV4	30.6	34.2	32.3	32.5	37.4	33.0
DRV5	36.9	33.8	37.3	35.2	34.5	33.5
DRV6	34.4	32.4	34.0	32.3	34.5	33.0
PI-naïve B[1]	36.2	36.2	33.1	33.9	33.2	33.6

[1] Data taken from Ref. #20

Table 2. Summary of the fractional occupancy of the four nominal states from DEER population analysis.

Constructs	**States**	**Relative Populations (±5%)**			
		Curled-Open	**Closed**	**Semi-open**	**Wide-open**
DRV1	unbound	31	21	13	35
	CaP2	18	20	41	21
	DRV	26	20	35	19
DRV2	unbound	15	21	37	27
	CaP2	9	30	37	24
	DRV	9	19	38	34
DRV3	unbound	27	61	5	7
	CaP2	7	77	10	6

	DRV	0	100	0	0
DRV4	unbound	37	26	22	15
	CaP2	41	31	17	11
	DRV	36	30	20	14
DRV5	unbound	19	30	40	11
	CaP2	13	38	35	14
	DRV	20	41	25	14
DRV6	unbound	19	44	37	0
	CaP2	18	61	21	0
	DRV	17	52	31	0
B[1]	Unbound	0	3	90	7
	CaP2	0	80	16	4
	DRV	0	87	13	0

[1] Data taken from Ref. #20

Although comparing the most probable distances shows trends in the changes of the conformational landscape, we can determine the fractional occupancy, *fi*, of each state by modelling the conformational ensemble of HIV-1 PR with four different conformations termed curled/tucked- open, closed, semi-open and wide-open (Figure 1), [19, 56, 57] where spin-labels at site K55C generate populations nominally centered at 25-30, 33, 36, and 40-45 Å; respectively. DEER distance profiles are hence re-constructed as a series of Gaussian shaped populations representative of the conformational landscape comprising four ensembles as shown in Figure 1 [56]. Population analysis of DEER distance profiles for all six DRV constructs in the absence of inhibitor (unbound form) and in the presence of inhibitors Ca-P2 (a non-hydrolysable substrate) and DRV are shown in Figure 4, with full details of the data analysis presented in Supporting Information Figures SI5-23. Table 2 summarizes the relative percentages of each conformation, with Table SI-2 providing values of the population means, breadths and errors. Figure 5 and Figure SI-24, plots these values graphically; clearly showing that each DRV construct has a conformational sampling profile that differs markedly from PI-naïve subtype B. By graphing the difference in each population of the DRV constructs relative to PI-naïve subtype B (Figure 5D), we can conclude that in the absence of inhibitor, each DRV construct relative to PI-naïve subtype B has less population of the semi-open state (P=0.001), with in all cases a concomitant increase of the closed (P= 0.01), and open-like states, where open-like is the sum of the curled/tucked-open, and wide-open populations (P=0.01, save DRV6 P = 0.185).

In the unbound form, all DRV constructs sample higher relative percentages of the open-like states (curled-open and wide-open) than PI-naïve subtype B. DRV1 and DRV2 occupy roughly 35 ± 5% and 27 ± 5% of a wide-open ensemble; respectively, and DRV5 and DRV6 each sample 19 ± 5% of a curled/tucked-open conformation. Whereas for unbound DRV3 and DRV4, curled/tucked-open conformation become the most populated states with fractional occupancies of 27 ± 5% and 36 ± 5%; respectively. Together, the DEER data for these DRV constructs contain populations of these open-like conformations at statistically significantly higher percentages what we observe for subtype B (7 ± 4% and 4 ± 4% for wide-open and curled-tucked; respectively) [14, 20], see Supplementary Information Tables SI3-6 for z-test analysis of data. In addition the breadth of the curled-tucked populations are quite broad for many constructs (8-11 Å, Table SI-2) possibly reflecting great heterogeneity in flap conformation or possibly even an instability of the dimer; although we did not pursue any thermal stability investigations, we infer this through the pH sensitivity of DRV1 and DRV3. Interestingly, DRV3 and DRV6 have a relatively high population of a closed-like state (61 ± 5%) centered near 33 Å . We have observed several other constructs containing single point or multiple amino acid substitutions, such as natural polymorphisms (NPs) or secondary mutations, that induce a conformation that strongly reflects the closed state [12, 14] and for the single point mutant A73V or L63P, we crystallized this protein in the absence of inhibitor and obtain a structure strongly resembling inhibitor closed form of the protease (PDB ID: 5T84).

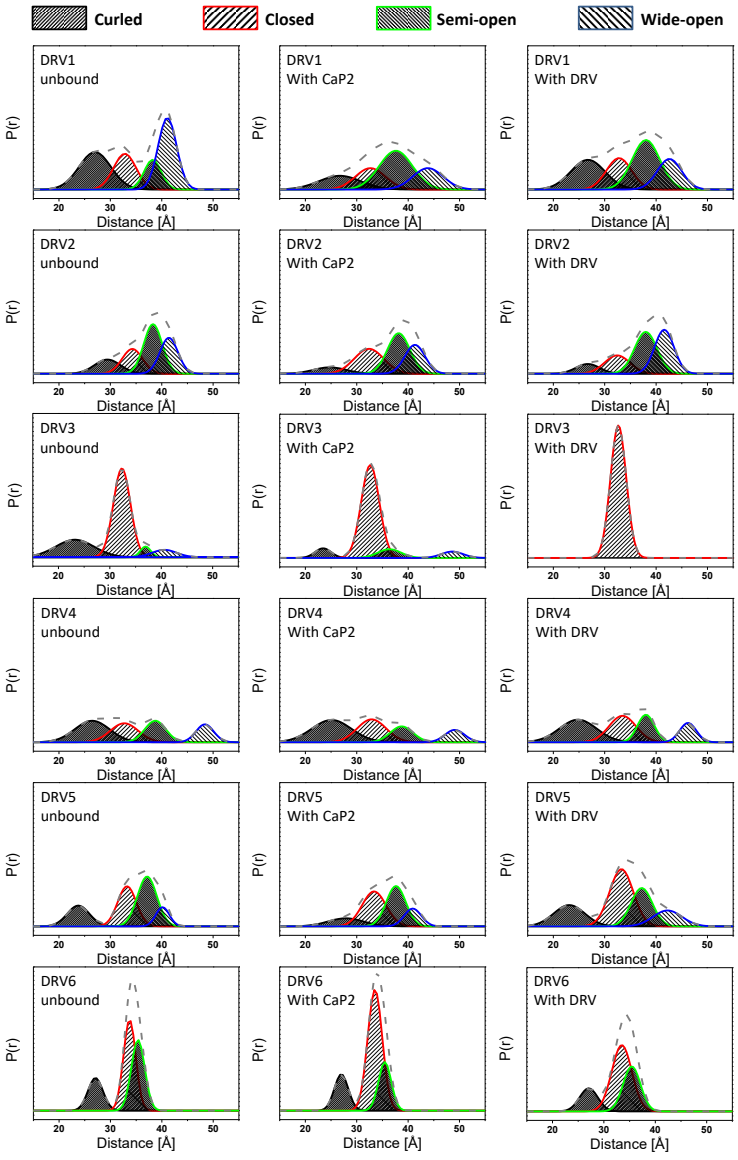

Figure 4. Population analysis of normalized DEER distance profiles for each construct in unbound, upon addition of non-hydrolysable CaP2 inhibitor or DRV inhibitor. The grey dashed line represents the overall population profile. The curled open conformation is rendered in black with tight forward hashes. The closed population is drawn with red with moderate spaced forward hashes. The semi-open conformation is represented by green line with tight back hash lines, and the wide-open conformation is in blue with moderately spaced back hash lines. Given the signal-to-noise ratio for collected DEER echo traces, error for populations is ± 3% P(r). Full details of data processing are given in supporting information and follow the protocol described previously [56, 57].

3.2. ***The conformational landscape of most DRV resistant constructs is not altered by addition of DRV or substrate mimic.***

Also given in Table 1 and Table 2 are the analysis of DEER results for DRV resistant constructs in the presence a non-hydrolysable substrate analog CaP2 or DRV. In most cases, except for DRV3, very little to no change in the distance probability profile is observed upon addition of these ligands. This effect can be seen in Figure 4 by comparing the DEER distance distribution profiles (that also contain the population analysis results) from left (unbound state) to right the middle panel (with CaP2) and the right panel (with DRV). In most cases, minor to no changes can be observed. For DRV3, however, the addition of CaP2 and DRV alter the conformational landscape by removing population density of the non-closed states, which is similar to the behavior of PI-naïve subtype B according to our previous studies [20].

Figures 5A-C plot the relative population (*i.e.*, the fractional occupancy) of each of the four states for each DRV construct in the absence and presence of inhibitor (either Ca-P2 or DRV). Figure 5D plots the relative difference in each fractional occupancy relative to PI-naïve subtype B for DRV constructs, showing there is a marked decrease in the inhibitor-induced closed population relative to PI-naïve subtype B for all DRV constructs except DRV3. These results are in stark contrast to many of our earlier studies where the CaP2 substrate analog usually bound to HIV-1 PR and shifted the conformational ensemble to nominally 98% or greater fractional occupancy of the closed state [13, 17, 19, 20]. Given the fold change in K_m values reported for these constructs (ranging from ~ 1-9x wild-type (WT) values) [31], it may not be surprising that we observed little to no conformational shift with CaP2. We do note that our constructs have the D25N mutation which may enhance this observed effect as it is known that the hydrogen bonding interaction of inhibitors with the active site add stabilization energy that is mitigated when the aspartic acid is replaced with an asparagine [16, 17] which has been shown to lower binding affinities by 100-1000 fold [59]. Nevertheless, in our earlier studies, except for when we characterized a construct that had a co-evolved substrate [12], CaP2 induced a strong shift to the closed state even with the D25N substitution. DRV3 showed the most dramatic alterations in the conformational landscape upon addition of CaP2 and DRV, where addition of these inhibitors removed the non-closed populations, similar to our earlier studies [14, 16, 17, 19, 20] This finding for DRV3 can be understood given that published kinetic and inhibition studies report K_m, k_{cat}/K_m and $\underline{K}_i$ values for inhibitors Lopinavir (LPV) and DRV) are most similar to PI-naïve subtype B compared to the other DRV analogs [31]. For other DRV constructs, little to no change in the DEER distance profile was observed upon addition of DRV; consistent with K_i values that ranged from ~32-2000x WT values [31].

3.3. ***Conformational Landscape Hypothesis for Catalytic Turnover is Upheld***

The conformational flexibility of HIV-1 PR is well known to be essential for kinetic activity [*[26]*]. Results from earlier DEER investigations on nelfinavir (NFV) resistant constructs suggested that the semi-open conformation is essential for catalytic turnover [14]. Figure 6A plots the relative ratio of the catalytic rate ($k_{cat\ (DRV)}/ k_{cat\ (WT)}$) for each construct as a function of the percentage of the semi-open conformation for the six DRV constructs. This figure also contains data obtained for the accumulated D30N/M36I/A71V NFV resistance mutations [14]. All of the DRV constructs have conformational landscapes that occupy < 50% of the semi-open conformation, which is significantly less than that seen in PI-naïve subtype B (Figure 5A and top panel of Figure 5D) and corresponds with catalytic turnover that is less than half that of the wild-type enzyme (Figure 6A). Numerous studies of DRV resistant constructs have reported consistent findings with enzymatic activity less than WT [34, 36, 38] The DEER population analysis reported here upholds a concept that enzymatic efficiency is obtained by a predominant (> 60%) semi-open conformation of protease, where the drug resistance

mutations combine to alter conformational sampling that corresponds well to the predicted correlation with kinetic activity [14].

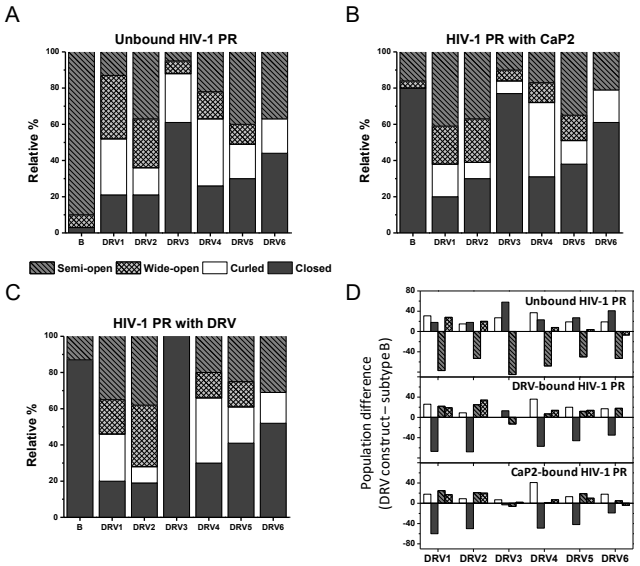

Figure 5. Graphical representation of the relative populations of each of the four conformational states for each HIV-1 PR construct in (A) an unbound state, (B) addition of the non-hydrolysable substrate analog Ca-P2, and (C) addition of inhibitor DRV. (D) plots the difference in the population of each state for each DRV construct relative to PI-naïve subtype B.

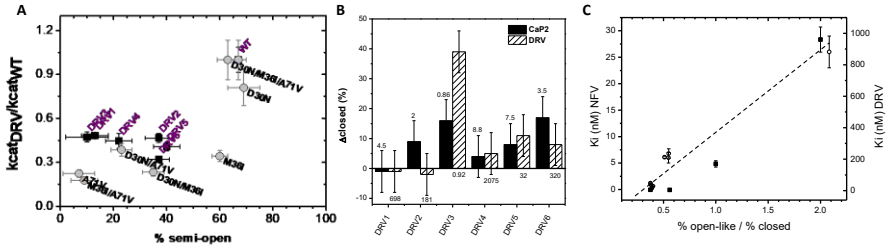

Figure 6. (A) Ratio of $kcat_{DRV}/kcat_{WT}$ for each construct versus the fractional occupancy of the semi-open conformation in unbound HIV-1 PR. Data are included for the 6 DRV constructs (black squares) as well as for a series of accumulated mutations in response to nelfinavir (NLV) (grey circles) – taken from Ref. #14. (B) Plot of the change in the closed population (Δclosed% = closed(inhibitor) – closed (unbound)) for each DRV construct with solid bars being the non-hydrolysable CaP2 inhibitor and slashed bars data for DRV inhibitor. Numbers above the bar report the fold change in K_m values, whereas numbers below the bars report the fold change in K_i values (data taken from Ref. # 31). (C) Plot of K_i value as a function of the fractional occupancy of the ratio of the open-like to closed states for unbound DRV constructs with K_i(DRV) plotted as solid squares compared to our earlier investigations of NFV resistant constructs to K_i(NLV) plotted as open circles. The dashed line is a guide for the eyes showing a linear trend. The y-axes differ for the two data sets and are labeled according to the inhibitor.

Figure 6B plots for each DRV construct the change in the fractional occupancy of the closed conformation, Dclosed, upon addition of CaP2 or DRV. Numbers on top of the bars reflect the fold change in K_m and those reported below the bars reflect the fold change in K_i. As expected, DRV3 has a marked conformational shift in the presence of inhibitor DRV. Other constructs have trends in the shift to the closed state that parallel kinetic and inhibition parameters; meaning as the fold change increases, less of a conformational shift is observed. These results are also seen in the data in Figure 5D for CaP2 and DRV bound showing that less of the closed population is observed compared to PI-naïve subtype B. Although we observed this relationship between the conformational shift and the fold change, the change in closed population is far from quantitative characterization of the fold change of K_i.

Figure 6C plots K_i values for DRV for the DRV constructs investigated here versus the ratio of the open-like population to closed state as we had done previously for a series of NFV accumulated mutations in subtype B [14]. We again find a correlation with the increase in the K_i values to stabilization of open-like states (open like = wide open + curled/tucked open) relative to the stability of the closed state. However, we should note that the relative changes in *K*i values have dramatically distinct and independent slopes (~15 nM for NFV-resistant PR vs. ~500 nM for DRV resistant PR), The current result together with our previous finding suggested the ratio of open-like to closed population as an alternative and uniform way to evaluate how conformational sampling can impact HIV-1 PR drug resistance

4. Discussion

There have been continued efforts to understand how mutations that accumulate distal from the active site in HIV-1 PR, and in other viral or cancer related proteins, alter enzymatic activity and impart resistance. For HIV-1 PR, others have indicated that some secondary mutations (i.e.; drug-pressure selected mutations that are not within the active site cavity) alter the manner in which the extended substrate interacts with PR, perhaps important in initial protease cleavage events [39]. It is also possible that distal mutations can impact dimerization or interactions with other HIV-1 or host proteins, including altering protease dynamics [24, 25, 27-29]. We have utilized both DEER and NMR spectroscopies to characterize how the accumulation of secondary drug-pressure selected mutations (which are also natural polymorphisms in other HIV-1PR clades) alter the conformational landscape and protein dynamics. The model emerging from our investigations utilizes the 4-state conformational landscape where mutations that stabilize closed states increase the rigidity of protease. In contrast, those mutations that lead to multi-drug resistance modulate the conformational landscape to stabilize the open-like states, destabilize the closed state, and increase overall protein backbone dynamics [12, 19] The fractional occupancy, f_i, of each state can be reflective of the relative thermodynamic stability Gibbs free energy, ΔG; where the more populated the state the more stable it is given by $\Delta G = -RT \ln f_i$

The investigations into these DRV resistant constructs uphold our earlier findings and lend further support to as conformational selection hypothesis. Interestingly, our earlier studies on the accumulation of mutations in response to NFV resulted in an enzyme with catalytic activity comparable to WT but resistant to > 3 inhibitors. For DRV resistance, we note that these accumulated mutations do not result in an enzyme with activity comparable to WT. Perhaps this arises because the sequences we investigated are not clinical isolates but rather generated from commonly seen DRV primary and secondary mutations. An additional explanation maybe that because DRV was designed to closely mimic the substrate envelop [32] such that evolving resistance would be difficult; it is reasonable that mutations that destabilize DRV binding may also compromise substrate binding – a result we see in our DEER data and reflected in published kinetic studies of others [31].

Supplementary Materials: The following are available online at www.mdpi.com/xxx/s1, Mass spectrometry analysis, Table S1: Summary of expected and observed mass for MTSL labeled HIV-1 PR constructs determined from mass spectrometry. Amino acid sequences of constructs utilized, Figure S1: Sequence alignment of constructs studied here title, Continuous Wave EPR spectra to evaluate sample quality, Figure S2. 100G CW X-

band EPR spectra for DRV3 HIV-1 PR (A) as a function of solution pH in20 mM D_3-NaOAc/D_2O, pH 5.0 with 30% v/v D_8-glycerol compared to spectrum obtained for WT (Bsi). Figure S3. Stack plot of 100G CW X-band EPR spectra for unbound HIV-1 PR DRV1 showing how pH alters spectra which is inferred as sample homogeneity. Dynamic light scattering, Figure S4**.** DLS results as a function of pH for DRV3 and DRV1 with and without DRV. DEER data and analysis for DRV1-6 unbound, with CaP2 and with DRV, Figures S5-23.

Author Contributions: Authors have contributed in the following capacities: Conceptualization, Gail E. Fanucci; Data curation, Zhanglong Liu, Trang T. Tran, Lingna Hu, Linh Pham and Kyle Bentz; Formal analysis, Zhanglong Liu, Trang T. Tran, Linh Pham and Daniel A. Savin; Funding acquisition, Gail E. Fanucci; Investigation, Zhanglong Liu and Gail E. Fanucci; Methodology, Daniel A. Savn and Gail E. Fanucci; Project administration, Gail E. Fanucci; Supervision, Daniel A. Savn and Gail E. Fanucci; Writing – original draft, Gail E. Fanucci; Writing – review & editing, Zhanglong Liu, Trang T. Tran and Linh Pham.

Funding: This work was supported by the National Institutes of Health S10RR031603 and GM105409 (G.E.F.) NIH (S10 OD021758-01) for ESI-MS (KB), National Science Foundation MCB-1715384 (G.E.F) and DMR-1709784 (D.A.S.), NHMFL-IHRP and NSF CRIF Grant 0541761,

Acknowledgments: We thank Dr. Alexander Angerhofer for maintenance of our shared EPR facility and Dr. Kari Basso for ESI data collection and helpful discussions.

Conflicts of Interest: "The authors declare no conflict of interest."

References

1. Kramer, R. A.; Schaber, M. D.; Skalka, A. M.; Ganguly, K.; Wong-Staal, F.; Reddy, E. P., HTLV-III gag protein is processed in yeast cells by the virus pol-protease. *Science (New York, N.Y.)* **1986,** 231, (4745), 1580-4.
2. Weber, I. T.; Miller, M.; Jaskolski, M.; Leis, J.; Skalka, A. M.; Wlodawer, A., Molecular Modeling of the Hiv-1 Protease and Its Substrate Binding-Site. *Science (New York, N.Y.)* **1989,** 243, (4893), 928-931. DOI 10.1126/science.2537531
3. Wlodawer, A.; Erickson, J. W., Structure-Based Inhibitors of Hiv-1 Protease. *Annu Rev Biochem* **1993,** 62, 543-585. DOI 10.1146/annurev.bi.62.070193.002551
4. Yin, P. D.; Das, D.; Mitsuya, H., Overcoming HIV drug resistance through rational drug design based on molecular, biochemical, and structural profiles of HIV resistance. *Cell Mol Life Sci* **2006,** 63, (15), 1706-1724. DOI 10.1007/s00018-006-6009-7
5. Lefebvre, E.; Schiffer, C. A., Resilience to resistance of HIV-1 protease inhibitors: Profile of darunavir. *Aids Rev* **2008,** 10, (3), 131-142.
6. Clutter, D. S.; Jordan, M. R.; Bertagnolio, S.; Shafer, R. W., HIV-1 drug resistance and resistance testing. *Infect Genet Evol* **2016,** 46, 292-307. 10.1016/j.meegid.2016.08.031
7. Wensing, A. M.; Calvez, V.; Gunthard, H. F.; Johnson, V. A.; Paredes, R.; Pillay, D.; Shafer, R. W.; Richman, D. D., 2017 Update of the Drug Resistance Mutations in HIV-1. *Top Antivir Med* **2016,** 24, (4), 132-133.
8. Feder, A. F.; Rhee, S. Y.; Holmes, S. P.; Shafer, R. W.; Petrov, D. A.; Pennings, P. S., More effective drugs lead to harder selective sweeps in the evolution of drug resistance in HIV-1. *Elife* **2016,** 5. 10.7554/eLife.10670
9. Jeschke, G.; Chechik, V.; Ionita, P.; Godt, A.; Zimmermann, H.; Banham, J.; Timmel, C. R.; Hilger, D.; Jung, H., DeerAnalysis2006 - A Comprehensive Software Package for Analyzing Pulsed ELDOR Data. *Appl. Mag. Reson.* **2006,** 30, 473-498.
10. Jeschke, G.; Polyhach, Y., Distance measurements on spin-labelled biomacromolecules by pulsed electron paramagnetic resonance. *Phys Chem Chem Phys* **2007,** 9, (16), 1895-1910.

11. Chiang, Y. W.; Borbat, P. P.; Freed, J. H., The determination of pair distance distributions by pulsed ESR using Tikhonov regularization. *J Magn Reson* **2005,** 172, (2), 279-95. S1090-7807(04)00353-2 [pii] 10.1016/j.jmr.2004.10.012
12. Carter, J. D.; Mathias, J. D.; Gomez, E. F.; Ran, Y.; Xu, F.; Galiano, L.; Tran, N. Q.; D'Amore, P. W.; Wright, C. S.; Chakravorty, D. K.; Fanucci, G. E., Characterizing Solution Surface Loop Conformational Flexibility of the GM2 Activator Protein. *J Phys Chem B* **2014,** 118, (36), 10607-10617. 10.1021/jp505938t
13. de Vera, I. M.; Blackburn, M. E.; Fanucci, G. E., Correlating conformational shift induction with altered inhibitor potency in a multidrug resistant HIV-1 protease variant. *Biochemistry* **2012,** 51, (40), 7813-5. 10.1021/bi301010z
14. de Vera, I. M.; Smith, A. N.; Dancel, M. C.; Huang, X.; Dunn, B. M.; Fanucci, G. E., Elucidating a relationship between conformational sampling and drug resistance in HIV-1 protease. *Biochemistry* **2013,** 52, (19), 3278-88. 10.1021/bi400109d
15. Galiano, L.; Ding, F.; Veloro, A. M.; Blackburn, M. E.; Simmerling, C.; Fanucci, G. E., Drug pressure selected mutations in HIV-1 protease alter flap conformations. *J Am Chem Soc* **2009,** 131, (2), 430-1. 10.1021/ja807531v 10.1021/ja807531v [pii]
16. Huang, X.; Britto, M. D.; Kear-Scott, J. L.; Boone, C. D.; Rocca, J. R.; Simmerling, C.; McKenna, R.; Bieri, M.; Gooley, P. R.; Dunn, B. M.; Fanucci, G. E., The role of select subtype polymorphisms on HIV-1 protease conformational sampling and dynamics. *J Biol Chem* **2014,** 289, (24), 17203-14. M114.571836 [pii] 10.1074/jbc.M114.571836
17. Huang, X.; de Vera, I. M.; Veloro, A. M.; Blackburn, M. E.; Kear, J. L.; Carter, J. D.; Rocca, J. R.; Simmerling, C.; Dunn, B. M.; Fanucci, G. E., Inhibitor-induced conformational shifts and ligand-exchange dynamics for HIV-1 protease measured by pulsed EPR and NMR spectroscopy. *J Phys Chem B* **2012,** 116, (49), 14235-44. 10.1021/jp308207h
18. Kear, J. L.; Blackburn, M. E.; Veloro, A. M.; Dunn, B. M.; Fanucci, G. E., Subtype polymorphisms among HIV-1 protease variants confer altered flap conformations and flexibility. *J Am Chem Soc* **2009,** 131, (41), 14650-1. 10.1021/ja907088a
19. Liu, Z.; Casey, T. M.; Blackburn, M. E.; Huang, X.; Pham, L.; de Vera, I. M.; Carter, J. D.; Kear-Scott, J. L.; Veloro, A. M.; Galiano, L.; Fanucci, G. E., Pulsed EPR characterization of HIV-1 protease conformational sampling and inhibitor-induced population shifts. *Phys Chem Chem Phys* **2016,** 18, (8), 5819-31. 10.1039/c5cp04556h
20. Blackburn, M. E.; Veloro, A. M.; Fanucci, G. E., Monitoring inhibitor-induced conformational population shifts in HIV-1 protease by pulsed EPR spectroscopy. *Biochemistry* **2009,** 48, (37), 8765-7. 10.1021/bi901201q
21. Wong-Sam, A.; Wang, Y. F.; Zhang, Y.; Ghosh, A. K.; Harrison, R. W.; Weber, I. T., Drug Resistance Mutation L76V Alters Nonpolar Interactions at the Flap-Core Interface of HIV-1 Protease. *ACS Omega* **2018,** 3, (9), 12132-12140. 10.1021/acsomega.8b01683
22. Louis, J. M.; Zhang, Y.; Sayer, J. M.; Wang, Y. F.; Harrison, R. W.; Weber, I. T., The L76V drug resistance mutation decreases the dimer stability and rate of autoprocessing of HIV-1 protease by reducing internal hydrophobic contacts. *Biochemistry* **2011,** 50, (21), 4786-95. 10.1021/bi200033z
23. Goldfarb, N. E.; Ohanessian, M.; Biswas, S.; McGee, T. D., Jr.; Mahon, B. P.; Ostrov, D. A.; Garcia, J.; Tang, Y.; McKenna, R.; Roitberg, A.; Dunn, B. M., Defective hydrophobic sliding mechanism and active site expansion in HIV-1 protease drug resistant variant Gly48Thr/Leu89Met: mechanisms for the loss of saquinavir binding potency. *Biochemistry* **2015,** 54, (2), 422-33. 10.1021/bi501088e

24. Ragland, D. A.; Nalivaika, E. A.; Nalam, M. N.; Prachanronarong, K. L.; Cao, H.; Bandaranayake, R. M.; Cai, Y.; Kurt-Yilmaz, N.; Schiffer, C. A., Drug resistance conferred by mutations outside the active site through alterations in the dynamic and structural ensemble of HIV-1 protease. *J Am Chem Soc* **2015,** 136, (34), 11956-63. 10.1021/ja504096m
25. Cai, Y.; Myint, W.; Paulsen, J. L.; Schiffer, C. A.; Ishima, R.; Kurt Yilmaz, N., Drug Resistance Mutations Alter Dynamics of Inhibitor-Bound HIV-1 Protease. *J Chem Theory Comput* **2014,** 10, (8), 3438-3448. 10.1021/ct4010454
26. Foulkes-Murzycki, J. E.; Scott, W. R.; Schiffer, C. A., Hydrophobic sliding: a possible mechanism for drug resistance in human immunodeficiency virus type 1 protease. *Structure* **2007,** 15, (2), 225-33. S0969-2126(07)00035-4 [pii] 10.1016/j.str.2007.01.006
27. Agniswamy, J.; Louis, J. M.; Roche, J.; Harrison, R. W.; Weber, I. T., Structural Studies of a Rationally Selected Multi-Drug Resistant HIV-1 Protease Reveal Synergistic Effect of Distal Mutations on Flap Dynamics. *PLoS One* **2016,** 11, (12), e0168616. 10.1371/journal.pone.0168616
28. Henes, M.; Lockbaum, G. J.; Kosovrasti, K.; Leidner, F.; Nachum, G. S.; Nalivaika, E. A.; Lee, S. K.; Spielvogel, E.; Zhou, S.; Swanstrom, R.; Bolon, D. N. A.; Kurt Yilmaz, N.; Schiffer, C. A., Picomolar to Micromolar: Elucidating the Role of Distal Mutations in HIV-1 Protease in Conferring Drug Resistance. *ACS Chem Biol* **2019,** 14, (11), 2441-2452. 10.1021/acschembio.9b00370
29. Laco, G. S., HIV-1 protease substrate-groove: Role in substrate recognition and inhibitor resistance. *Biochimie* **2015,** 118, 90-103. 10.1016/j.biochi.2015.08.009
30. Clemente, J. C.; Hemrajani, R.; Blum, L. E.; Goodenow, M. M.; Dunn, B. M., Secondary mutations M36I and A71V in the human immunodeficiency virus type 1 protease can provide an advantage for the emergence of the primary mutation D30N. *Biochemistry* **2003,** 42, (51), 15029-35. 10.1021/bi035701y
31. Saskova, K. G.; Kozisek, M.; Rezacova, P.; Brynda, J.; Yashina, T.; Kagan, R. M.; Konvalinka, J., Molecular characterization of clinical isolates of human immunodeficiency virus resistant to the protease inhibitor darunavir. *J Virol* **2009,** 83, (17), 8810-8. JVI.00451-09 [pii] 10.1128/JVI.00451-09
32. Altman, M. D.; Ali, A.; Reddy, G. S.; Nalam, M. N.; Anjum, S. G.; Cao, H.; Chellappan, S.; Kairys, V.; Fernandes, M. X.; Gilson, M. K.; Schiffer, C. A.; Rana, T. M.; Tidor, B., HIV-1 protease inhibitors from inverse design in the substrate envelope exhibit subnanomolar binding to drug-resistant variants. *J Am Chem Soc* **2008,** 130, (19), 6099-113. 10.1021/ja076558p
33. Zhang, Y.; Chang, Y. C.; Louis, J. M.; Wang, Y. F.; Harrison, R. W.; Weber, I. T., Structures of darunavir-resistant HIV-1 protease mutant reveal atypical binding of darunavir to wide open flaps. *ACS Chem Biol* **2014,** 9, (6), 1351-8. 10.1021/cb4008875
34. Weber, I. T.; Kneller, D. W.; Wong-Sam, A., Highly resistant HIV-1 proteases and strategies for their inhibition. *Future Med Chem* **2015,** 7, (8), 1023-38. 10.4155/fmc.15.44
35. Kurt Yilmaz, N.; Swanstrom, R.; Schiffer, C. A., Improving Viral Protease Inhibitors to Counter Drug Resistance. *Trends Microbiol* **2016,** 24, (7), 547-57. S0966-842X(16)30002-6 [pii] 10.1016/j.tim.2016.03.010
36. Kneller, D. W.; Agniswamy, J.; Ghosh, A. K.; Weber, I. T., Potent antiviral HIV-1 protease inhibitor combats highly drug resistant mutant PR20. *Biochem Biophys Res Commun* **2019,** 519, (1), 61-66. 10.1016/j.bbrc.2019.08.126
37. Agniswamy, J.; Kneller, D. W.; Brothers, R.; Wang, Y. F.; Harrison, R. W.; Weber, I. T., Highly Drug-Resistant HIV-1 Protease Mutant PRS17 Shows Enhanced Binding to Substrate Analogues. *ACS Omega* **2019,** 4, (5), 8707-8719. 10.1021/acsomega.9b00683

38. Pawar, S. D.; Freas, C.; Weber, I. T.; Harrison, R. W., Analysis of drug resistance in HIV protease. *BMC Bioinformatics* **2018,** 19, (Suppl 11), 362. 10.1186/s12859-018-2331-y
39. Humpolickova, J.; Weber, J.; Starkova, J.; Masinova, E.; Gunterova, J.; Flaisigova, I.; Konvalinka, J.; Majerova, T., Inhibition of the precursor and mature forms of HIV-1 protease as a tool for drug evaluation. *Sci Rep* **2018,** 8, (1), 10438. 10.1038/s41598-018-28638-w
40. Lockbaum, G. J.; Leidner, F.; Rusere, L. N.; Henes, M.; Kosovrasti, K.; Nachum, G. S.; Nalivaika, E. A.; Ali, A.; Yilmaz, N. K.; Schiffer, C. A., Structural Adaptation of Darunavir Analogues against Primary Mutations in HIV-1 Protease. *ACS Infect Dis* **2019,** 5, (2), 316-325. 10.1021/acsinfecdis.8b00336
41. Matthew, A. N.; Leidner, F.; Newton, A.; Petropoulos, C. J.; Huang, W.; Ali, A.; KurtYilmaz, N.; Schiffer, C. A., Molecular Mechanism of Resistance in a Clinically Significant Double-Mutant Variant of HCV NS3/4A Protease. *Structure* **2018,** 26, (10), 1360-1372 e5. 10.1016/j.str.2018.07.004
42. Khan, S. N.; Persons, J. D.; Paulsen, J. L.; Guerrero, M.; Schiffer, C. A.; Kurt-Yilmaz, N.; Ishima, R., Probing Structural Changes among Analogous Inhibitor-Bound Forms of HIV-1 Protease and a Drug-Resistant Mutant in Solution by Nuclear Magnetic Resonance. *Biochemistry* **2018,** 57, (10), 1652-1662. 10.1021/acs.biochem.7b01238
43. Lockbaum, G. J.; Leidner, F.; Rusere, L. N.; Henes, M.; Kosovrasti, K.; Nachum, G. S.; Nalivaika, E. A.; Bolon, D. N. A.; Ali, A.; Kurt Yilmaz, N.; Schiffer, C. A., Correction to Structural Adaptation of Darunavir Analogues against Primary Mutations in HIV-1 Protease. *ACS Infect Dis* **2019,** 5, (6), 1044. 10.1021/acsinfecdis.9b00098
44. Agniswamy, J.; Shen, C. H.; Wang, Y. F.; Ghosh, A. K.; Rao, K. V.; Xu, C. X.; Sayer, J. M.; Louis, J. M.; Weber, I. T., Extreme multidrug resistant HIV-1 protease with 20 mutations is resistant to novel protease inhibitors with P1'-pyrrolidinone or P2-tris-tetrahydrofuran. *J Med Chem* **2013,** 56, (10), 4017-27. 10.1021/jm400231v
45. Agniswamy, J.; Shen, C. H.; Aniana, A.; Sayer, J. M.; Louis, J. M.; Weber, I. T., HIV-1 protease with 20 mutations exhibits extreme resistance to clinical inhibitors through coordinated structural rearrangements. *Biochemistry* **2012,** 51, (13), 2819-28. 10.1021/bi2018317
46. Kozisek, M.; Lepsik, M.; Grantz Saskova, K.; Brynda, J.; Konvalinka, J.; Rezacova, P., Thermodynamic and structural analysis of HIV protease resistance to darunavir - analysis of heavily mutated patient-derived HIV-1 proteases. *FEBS J* **2014,** 281, (7), 1834-47. 10.1111/febs.12743
47. Mildner, A. M.; Rothrock, D. J.; Leone, J. W.; Bannow, C. A.; Lull, J. M.; Reardon, I. M.; Sarcich, J. L.; Howe, W. J.; Tomich, C. S.; Smith, C. W., The HIV-1 protease as enzyme and substrate: mutagenesis of autolysis sites and generation of a stable mutant with retained kinetic properties. *Biochemistry* **1994,** 33, (32), 9405-13.
48. Galiano, L.; Bonora, M.; Fanucci, G. E., Interflap distances in HIV-1 protease determined by pulsed EPR measurements. *J Am Chem Soc* **2007,** 129, (36), 11004-5. 10.1021/ja073684k
49. Shao, W.; Everitt, L.; Manchester, M.; Loeb, D. D.; Hutchison, C. A., 3rd; Swanstrom, R., Sequence requirements of the HIV-1 protease flap region determined by saturation mutagenesis and kinetic analysis of flap mutants. *Proc Natl Acad Sci U S A* **1997,** 94, (6), 2243-8. 10.1073/pnas.94.6.2243
50. Galiano, L.; Blackburn, M. E.; Veloro, A. M.; Bonora, M.; Fanucci, G. E., Solute effects on spin labels at an aqueous-exposed site in the flap region of HIV-1 protease. *J Phys Chem B* **2009,** 113, (6), 1673-80. 10.1021/jp8057788
51. Carter, J. D.; Gonzales, E. G.; Huang, X.; Smith, A. N.; de Vera, I. M.; D'Amore, P. W.; Rocca, J. R.; Goodenow, M. M.; Dunn, B. M.; Fanucci, G. E., Effects of PRE and POST therapy drug-pressure selected

mutations on HIV-1 protease conformational sampling. *FEBS Lett* **2014,** 588, (17), 3123-8. 10.1016/j.febslet.2014.06.051

52. Liu, Z.; Huang, X.; Hu, L.; Pham, L.; Poole, K. M.; Tang, Y.; Mahon, B. P.; Tang, W.; Li, K.; Goldfarb, N. E.; Dunn, B. M.; McKenna, R.; Fanucci, G. E., Effects of Hinge-region Natural Polymorphisms on Human Immunodeficiency Virus-Type 1 Protease Structure, Dynamics, and Drug Pressure Evolution. *J Biol Chem* **2016,** 291, (43), 22741-22756. 10.1074/jbc.M116.747568

53. Ding, F.; Layten, M.; Simmerling, C., Solution structure of HIV-1 protease flaps probed by comparison of molecular dynamics simulation ensembles and EPR experiments. *J Am Chem Soc* **2008,** 130, (23), 7184-5. 10.1021/ja800893d

54. Louis, J. M.; Clore, G. M.; Gronenborn, A. M., Autoprocessing of HIV-1 protease is tightly coupled to protein folding. *Nat Struct Biol* **1999,** 6, (9), 868-75. 10.1038/12327

55. Kear, J. L.; Galiano, L.; Veloro, A. M.; Harris, J.; Busenlehner, L. S.; Fanucci, G. E., Monitoring the autoproteolysis of HIV-1 Protease by Site-Directed Spin-Labeling and Electron Paramagnetic Resonance Spectroscopy. *J. Biophys. Chem.* **2011,** 2, (2), 137-146.

56. Casey, T. M.; Fanucci, G. E., Spin labeling and Double Electron-Electron Resonance (DEER) to Deconstruct Conformational Ensembles of HIV Protease. *Methods Enzymol* **2015,** 564, 153-87. S0076-6879(15)00423-1 [pii] 10.1016/bs.mie.2015.07.019

57. De Vera, I. M.; Blackburn, M. E.; Galiano, L.; Fanucci, E., Pulsed EPR distance measurements in soluble proteins by site-directed spin labeling (SDSL). *Curr Prot Protein Sci* **2013,** 74, 17.17. doi: 10.1002/0471140864

58. Tran, T. T.; Liu, Z.; Fanucci, G. E., Conformational landscape of non-B variants of HIV-1 protease: A pulsed EPR study. *Biochem Biophys Res Commun* **2020,** 532, (2), 219-224. 10.1016/j.bbrc.2020.08.030

59. Sayer, J. M.; Liu, F.; Ishima, R.; Weber, I. T.; Louis, J. M., Effect of the active site D25N mutation on the structure, stability, and ligand binding of the mature HIV-1 protease. *J Biol Chem* **2008,** 283, (19), 13459-70. 10.1074/jbc.M708506200